WAVE AND CURRENT INTERACTIONS WITH VEGETATION

TAKAO OTA

Dept. of Social Systems Eng., Tottori University, 4-101 Koyama Minami Tottori, 680-8552, Japan

NOBUHISA KOBAYASHI

Center for Applied Coastal Research, University of Delaware, Newark DE 19716, USA

JAMES T. KIRBY

Center for Applied Coastal Research, University of Delaware, Newark, DE 19716, USA

The characteristics of currents, waves and turbulent velocities in and above submerged vegetation and the resulting wave attenuation are examined in a series of laboratory experiments and using simple theoretical models based on the mixing layer analogy for vegetated flows, the time-averaged momentum equation including the horizontal drag force, and linear wave theory.

1. Introduction

Aquatic vegetation is beneficial in the coastal ecosystem and reduces waves, currents and sand drift in the coastal environment. The wave attenuation by vegetation and the flow in and above the vegetation were investigated experimentally and analytically to predict the wave height decay and the flow field (Asano et al. 1992; Kobayashi et al. 1993; Mendez et al. 1999; Tamura and Nadaoka, 2002). Moreover, the hydraulic characteristics of vegetation in open channel flows have been investigated extensively in relation to the transport of sediment, nutrients and contaminants (Murota and Fukuhara, 1983; Shimizu and Tsujimoto, 1994; Nepf and Vivoni, 2000). However, the effects of vegetation on the combined wave and current field, which is more typical in the coastal environment, have never been examined probably because of the complexity of interactions among currents, waves and vegetation. In this study, the flow characteristics above and inside submerged vegetation and the resulting wave attenuation are investigated experimentally and analytically.

2. Experiments

Laboratory experiments were conducted in a 30-m-long, 0.6-m-wide, 0.8-m-deep

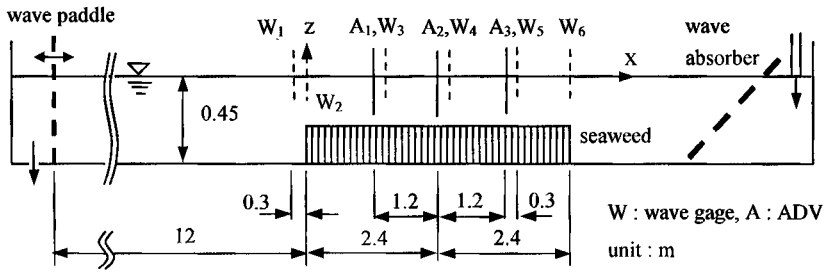

Fig. 1. Experimental setup

wave and recirculating flume. The experimental setup for the first experiment is shown in Fig. 1. Six wave gages and three acoustic Doppler velocimeters (ADV, 3-D) were used to measure the free surface elevation and the fluid velocities. The artificial seaweed was made of a 6-mm wide, 0.1-mm thick polyester blade. Each plant consists of four blades and was fixed to an 18-mm thick acrylic board. The number of plants per unit horizontal area was $N=0.1cm^{-2}$. The water depth and wave period of the incident regular waves were 45cm, and 1.4s or 2.0s, respectively. The direction of the current was opposite to the wave propagation. The measurement was started more than 30 minutes after the generation of the current and 3 minutes after the wave generation. 328-second time series were collected at a sampling rate of 25Hz for the wave gages and ADVs. The horizontal coordinate x is positive in the wave direction with x=0 at the seaward edge of the vegetation. The vertical coordinate z is taken to be positive upward with z=0 at the still water level. The ADVs were set at z=-13.2, -19.2, -25.2cm for the first experiment. In the second experiment, the velocities were measured in the center of the vegetation (x=2.4m) over the entire depth at a 2cm interval and the free surface elevation was measured at x=0, 1.2, 2.4, 3.6, 4.8m by using five pairs of wave gages as shown in Fig. 2. The average positions

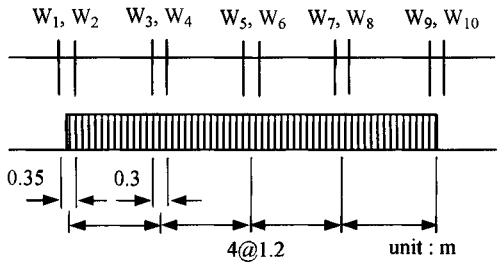

Fig. 2. Experimental setup (additional experiment)

Table 1. Average position of the seaweed top

	period (s)	h (cm)	d (cm)
current	N/A	27.5	15.7
wave	1.4	30.2	13.0
	2.0	28.5	14.7
wave and current	1.4	28.0	15.2
	2.0	25.4	17.8

of the top of seaweed measured on the video image are shown Table 1, where h and d denote the average water depth above the seaweed and the seaweed height from the bottom, respectively. It is noted that (h+d)=43.2 because of the 18-mm thick board.

3. Comparison of experimental results with current and wave models

3.1. *Current Model*

The horizontal time-averaged momentum equation is given by

$$\frac{\partial \tau_c}{\partial z} = \rho g s + \overline{F_x} \quad ; \quad -(h+d) \le z \le 0 \tag{1}$$

where τ_c = Reynolds stress, ρ = density of water, g = gravitational acceleration, s = slope ($\partial \overline{\eta} / \partial x$) of the mean water level, $\overline{\eta}$. $\overline{F_x}$ is the horizontal drag force acting on the vegetation and expressed as

$$\overline{F_x} = \frac{1}{2} \rho C_D b N P_v | u_c | u_c \tag{2}$$

where C_D = drag coefficient, b = seaweed width, N = 0.1cm^{-2}, and u_c = horizontal fluid velocity. P_v is the existence probability of seaweed at the elevation z for the swaying seaweed introduced to avoid sudden changes of the velocity and turbulence at the interface. In this paper, the probability distribution for the elevation of the seaweed top is assumed to follow the normal distribution with its standard deviation σ_v. Thus, P_v is expressed as

$$P_v(z) = \int_z^{\infty} \frac{1}{\sqrt{2\pi}\sigma_v} \exp\left\{ -\frac{1}{2}\left(\frac{z+h}{\sigma_v} \right)^2 \right\} dz = \frac{1}{2} erfc\left(\frac{z+h}{\sqrt{2}\,\sigma_v} \right) \tag{3}$$

where erfc = error function and the seaweed top is located at z=-h on the average. As shown in Fig. 3, the region affected by the swaying seaweed extends further upward as σ_v increases.

The hyperbolic tangent profile of a plane mixing layer (Ho and Huerre, 1984) is used for the mean

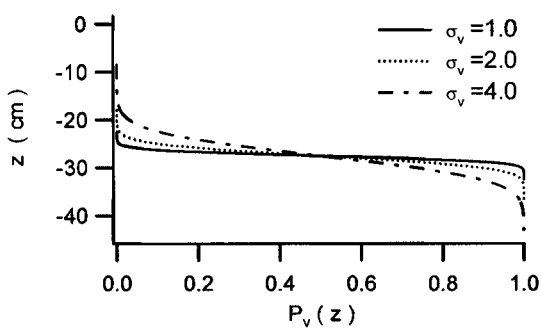

Fig. 3. Existence probability of seaweed at z

velocity profile in the same manner as Ghisalberti and Nepf (2002).

$$\frac{U-\overline{U}}{\Delta U}=\frac{1}{2}\tanh\left(\frac{z-\bar{z}}{2\theta}\right)\ ;\ \Delta U=U_2-U_1\ ,\overline{U}=(U_1+U_2)/2 \tag{4}$$

where U_1 and U_2 = uniform velocities of the upper and lower layer of the mixing layer ($U_2 > U_1$), $\bar{z}$ = elevation at which the velocity is equal to $\overline{U}$, and θ= momentum thickness of the mixing layer defined as

$$\theta=\int_{-\infty}^{\infty}\left\{\frac{1}{4}-\left(\frac{U-\overline{U}}{\Delta U}\right)^2\right\}\,dz \tag{5}$$

For the present experiment, we set $U_1=0$, $\overline{U}=U_2/2=u_i$, $U=u_c$ and $-\bar{z}=h_i$ in Eq. (4) where the subscript i denotes the inflection point. The mean current velocity profile is expressed as

$$\frac{u_c}{u_i}=1+\tanh\left(\frac{z+h_i}{2\theta}\right) \tag{6}$$

where θ and h_i are estimated semi-empirically as

$$\theta=\max\left[h/(\alpha+\beta),\ d/(\alpha-\beta)\right]\ ,\ h_i=h-\beta\theta \tag{7}$$

where α is the ratio between h_i and θ, and $\beta=(h-h_i)/\theta$. It is noted that θ is limited by the free surface and bottom unlike Eq. (5). We adopted $\alpha=5$ and $\beta=0.4$ for the values of h and d in Table 1. Integration of Eq. (1) with respect to z using Eq. (6) and assuming $\tau_c=0$ at $z=-(d+h)$ yields

$$\tau_c(z)=\rho g s z-\rho C_D b N\theta\left|u_i\right|u_i F(r) \tag{8}$$

$$u_i=-\left[\frac{gs(d+h)}{C_D bN\theta F(r_b)}\right]^{1/2}\quad ;\quad s>0 \tag{9}$$

where $r=-(z+h_i)/(2\theta)$, r_b = value of r at $z=-(d+h)$, and $s>0$ means that the mean water level increases in the positive direction of x. F(r) is given by

$$F(r)=\frac{1}{2}\int_{r_0}^{r} erfc\left[\frac{\delta}{\sqrt{2}}\left(1-\frac{2r}{\beta}\right)\right]\left[1-\tanh(r)\right]^2\,dr \tag{10}$$

where $\delta=(h-h_i)/\sigma_v$ is estimated empirically. Substitution of Eq. (9) into (8) yields

$$\frac{\tau_c}{\rho} = gs\left\{ z + (d+h)\frac{F(r)}{F(r_b)} \right\} \tag{11}$$

where τ_c is negative for opposing currents.

Fig. 4 shows the measured and predicted current velocity u_c with δ=1.0 and the measured slope s=0.000523 in Eqs. (9) and (10) based on the experimental result. The vertical profile of the measured current velocity agrees well with the

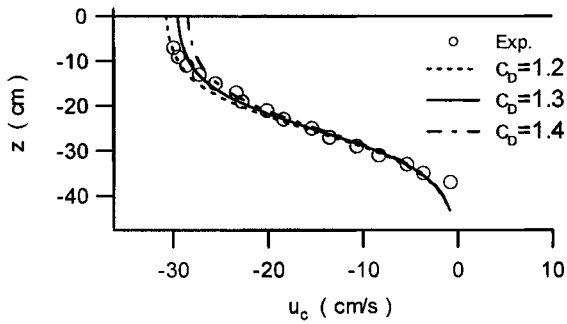

Fig. 4. Current velocity

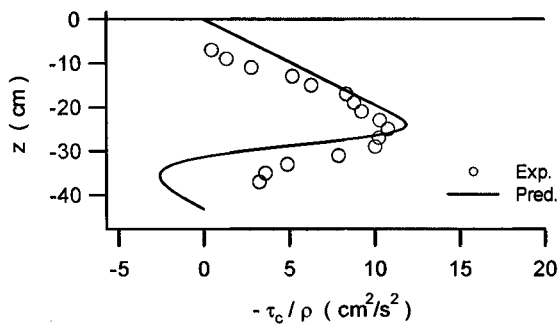

Fig. 5. Reynolds stress

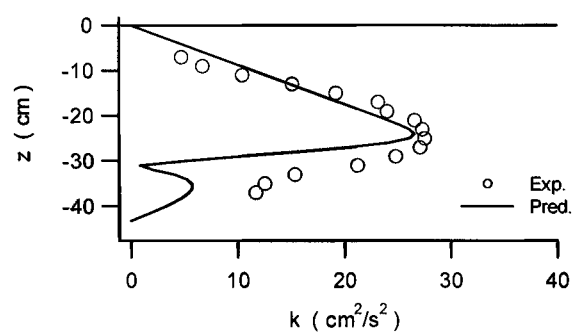

Fig. 6. Turbulent kinetic energy

velocity distribution of the mixing layer with C_D=1.3. Figs. 5 and 6 compare the Reynolds stress and the turbulent kinetic energy obtained as

$$\tau_c = -\rho\,\overline{u'w'} \quad ; \quad k = \frac{1}{2}\left(\overline{u'^2} + \overline{v'^2} + \overline{w'^2}\right) = \frac{|\tau_c|}{\rho\sqrt{C_d}} \tag{12}$$

where u', v' and w' = measured turbulent velocity components in the x, y and z directions, C_d = an empirical coefficient calibrated as 0.2 in this case. Eq. (11) and the relationship between k and $|\overline{\tau_c}|$ in Eq. (12) yield good agreement except in the lower layer of vegetation.

3.2. *Wave Model*

Kobayashi et al. (1993) developed a linear theory for wave attenuation due to submerged vegetation assuming that the wave height decays exponentially and the effects of vegetation on the flow field can be expressed in terms of the horizontal drag force. The exponential decay coefficient k_i is given by

$$\frac{k_i}{k_r} = \frac{\sqrt{8}C_D b N \sigma_0}{9\pi} \frac{\sinh(3k_r d) + 9\sinh(k_r d)}{\sinh[k_r(h+d)]\{2k_r(h+d) + \sinh[2k_r(h+d)]\}} \tag{13}$$

where k_r = real wave number, σ_0 = standard deviation of the free surface oscillation at x=0. Fig. 7 shows the measured standard deviation σ_η in comparison with the predicted exponential decay expressed as

$$\sigma_\eta(x) = \sigma_0 \exp(-k_i x) \tag{14}$$

The measured values of σ_η denoted by the open square and circle are the average of σ_η at the paired wave gages shown in Fig. 2. The fitted lines are the linear regression based on the least-squares method and Eq. (14). The predicted lines are based on Eq. (13) with C_D=1.3. The experimental and predicted values of k_i are 0.0283m^{-1}and 0.0340m^{-1} for the wave period T=1.4s, and 0.0458m^{-1} and 0.0545m^{-1} for T=2.0s respectively. Eq. (13) slightly overpredicts k_i for the drag coefficient C_D=1.3 calibrated for the current model above.

Fig. 8 shows the wave and turbulent velocity components in the wave field obtained using a phase-averaging method with the measured time series of 50 waves. The turbulent components are small and only the dominant wave components are analyzed. Based on linear wave theory without taking account of the vegetation, the standard deviations σ_u and σ_w of the horizontal and vertical velocities are expressed as

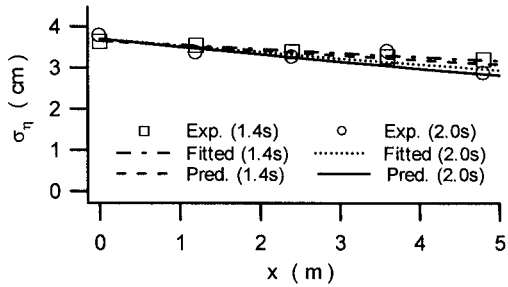

Fig. 7. Wave attenuation

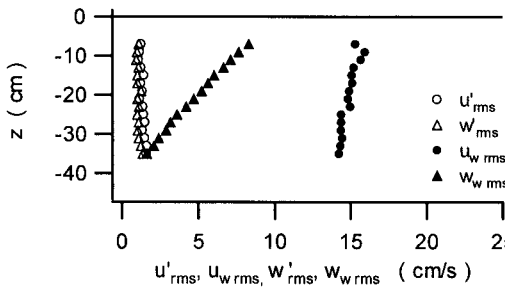

Fig. 8. Wave and turbulent velocity components

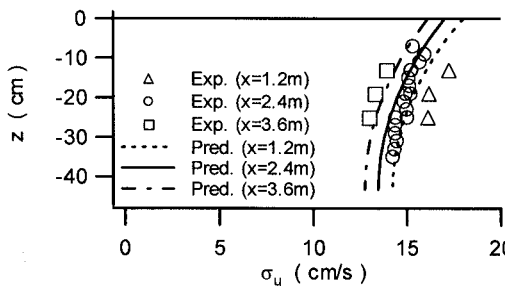

Fig. 9. Horizontal wave velocity components (T=2.0s)

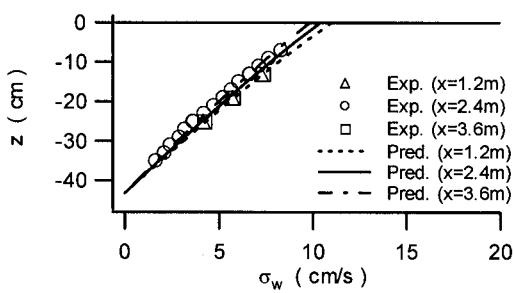

Fig. 10. Vertical wave velocity components (T=2.0s)

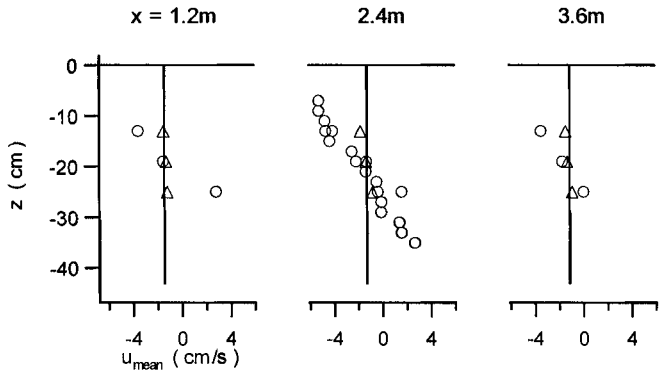

Fig. 11. Wave-induced mean velocity

$$\sigma_u(x,z) = \sigma_\eta(x)\frac{gk_r}{\omega}\frac{\cosh[k_r(z+d+h)]}{\cosh[k_r(d+h)]}$$

$$\sigma_w(x,z) = \sigma_\eta(x)\frac{gk_r}{\omega}\frac{\sinh[k_r(z+d+h)]}{\cosh[k_r(d+h)]} \tag{15}$$

where ω = angular frequency. Figs. 9 and 10 illustrate the measured and predicted σ_u and σ_w at x=1.2, 2.4, 3.6m for T=2.0s. The agreement is fairly good because the local effect of the vegetation on the wave velocity field is small unlike the current and vegetation interaction shown in Figs. 4-6.

Fig. 11 shows the wave-induced mean velocity at x=1.2, 2.4, 3.6m for T=2.0s. The open circles and triangles are the measured values with and without the vegetation, respectively, and the solid line is the return current in the absence of the vegetation given by

$$\overline{u}(x) = -\frac{gk_r\sigma_\eta^2(x)}{\omega(d+h)} \tag{16}$$

The measured wave-induced current is almost uniform in the case of no vegetation. In the presence of the vegetation, the direction of the flow is opposite to the wave propagation above the vegetation and in the same direction as the wave inside the vegetation. However, the measured velocity agrees with Eq. (16) on the average.

3.3. *Current and Wave Model*

The current and wave model is developed combining the current and wave models described above. The momentum equation (1) is assumed to be valid if

Eq. (2) is modified as

$$\overline{F_x} = \frac{1}{2}\rho C_D b N P_v \overline{|u_c + u_w|(u_c + u_w)} \tag{17}$$

where the overbar indicates time averaging and the wave horizontal velocity $u_w = \sqrt{2}\sigma_u \cos(\omega t)$ with σ_u = standard deviation. Integration of Eq. (1) with Eq. (17) assuming τ_c=0 at z=-(d+h) yields the same equations as Eqs. (8) and (9). However, F(r) is different from Eq. (10) and expressed as

$$F(r) = \frac{1}{2}\int_{r_0}^{r} erfc\left[\frac{\delta}{\sqrt{2}}\left(1-\frac{2r}{\beta}\right)\right] G(r)\ dr \quad ; \quad r_0 \le r \le r_b \tag{18}$$

where

$$G(r) = \begin{cases} a^2 + b^2/2 \ ; & a \ge |b| \\ a^2 + b^2/2 - [2\theta_0 a^2 - 4a|b|\sin\theta_0 + b^2(\theta_0 + 0.5\sin 2\theta_0)]/\pi \ ; & a < |b| \end{cases}$$

with $a = 1 - \tanh(r)$, $b = \sqrt{2}\sigma_u / u_i$, $\theta_0 = \cos^{-1}(a/|b|)$. The standard deviation σ_u of the horizontal wave velocity in the presence of the current is

$$\sigma_u(x,z) = \frac{g\sigma_\eta(x)}{C - U_c}\frac{\cosh[k_r(z+d+h)]}{\cosh[k_r(d+h)]} \tag{19}$$

where C = wave phase velocity, U_c = depth-averaged current velocity obtained using Eq. (6).

$$U_c = \frac{1}{d+h}\int_{-(d+h)}^{0} u_c\ dz = u_i\left\{1 - \frac{2\theta}{d+h}\ln\left[\frac{\cosh(r_b)}{\cosh(r_0)}\right]\right\} \tag{20}$$

The wave number k_r in Eq. (19) includes the effect of the current and should satisfy the following dispersion relation.

$$(C - U_c)^2 = g\tanh[k_r(h+d)]/k_r \tag{21}$$

An iterative calculation is necessary to determine u_i and U_c using Eqs. (9) and (18)-(21). Figs. 12 and 13 show the profiles of the mean horizontal velocity and Reynolds stress in the current and wave field. The open circles denote the measured values at x=2.4m for T=2.0s and the solid line is the prediction with C_D=0.6 and s=0.00116 (the measured mean waterlevel slope). The computed u_i and U_c are -17.4cm/s and -18.9cm/s for the opposing current. The use of C_D=1.3 results in the underestimation. The dotted line in Fig. 13 shows the profile obtained from the current model and agrees well with the experimental result,

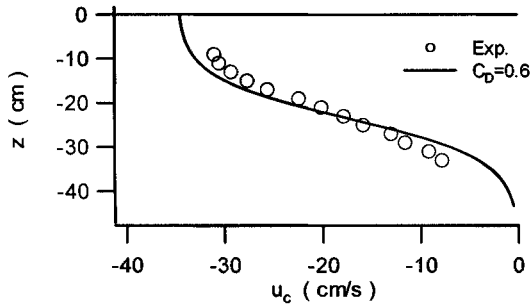

Fig. 12. Mean horizontal velocity

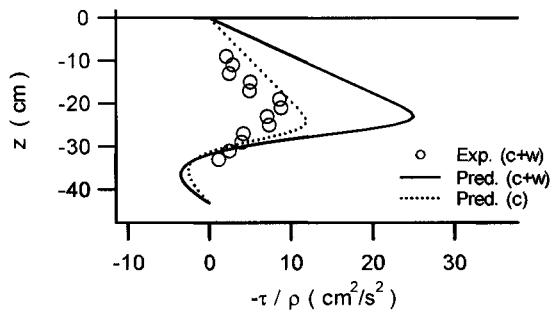

Fig. 13. Reynolds stress in the current and wave field

implying that the turbulence is affected little by the wave. The value of s has a significant effect in Eq. (11). The values of s for the current field and the current and wave field are different but the profiles of the Reynolds stress are very similar. The difference causes the disagreement in Fig. 13. The increase of s by a factor of about 2 due to the addition of the wave will need to be explained physically.

As for the wave attenuation, the measured values of σ_0 and k_i are 5.50cm and $0.0575m^{-1}$ for T=1.4s, and 4.89cm and $0.0508m^{-1}$ for T=2.0s. We derived an equation for the exponential decay coefficient k_i in the current and wave field by extending the model of Kobayashi et al. (1993).

$$\frac{k_i}{k_r} = \frac{C_D b N \sigma_0 I}{\sqrt{2}\left(n + \dfrac{U_c}{C - U_c}\right)\tanh^2 [k_r (d+h)]} \tag{22}$$

where

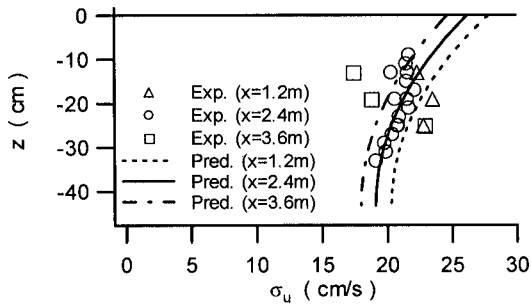

Fig. 14. Horizontal wave velocity components (T=2.0s, current+wave)

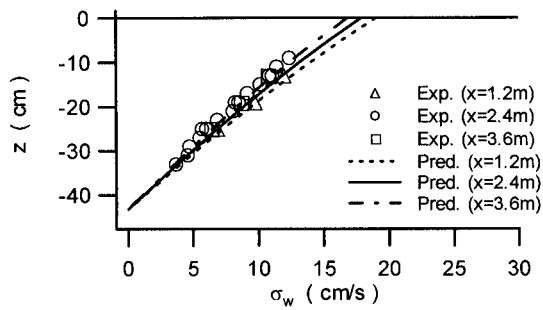

Fig. 15. Vertical wave velocity components (T=2.0s, current+wave)

$$n=\frac{1}{2}\left\{1+\frac{2k_r(d+h)}{\sinh[2k_r(d+h)}\right\}\ ,\quad I=\int_{-(d+h)}^{-h}\frac{\cosh^3[k_r(z+d+h)]}{\cosh^3[k_r(d+h)]}J(z)\,k_r\,dz\ ,$$

$$J(z)=\begin{cases}|a|^3+1.5|a| & ;\ |a|\geq 1\\ [a^3(2\theta_0-\pi)+6a^2\sin\theta_0+1.5a(2\theta_0-\pi+\sin 2\theta_0)\\ \quad +2\sin\theta_0-(2/3)\sin^3\theta_0]/\pi & ;\ |a|<1\end{cases}$$

with $a=u_c/(\sqrt{2}\sigma_u)$, $\theta_0=\cos^{-1}(-a)$; $0<\theta_0<\pi$. The predicted k_i for T=2.0s using Eq. (22) with C_D=1.3 and U_c=-20cm/s is 0.0933m^{-1} and almost twice of the measured value. The drag coefficient C_D=1.3 obtained from the current data is too large for the current and wave field. This suggests that it is difficult to describe the effect of the vegetation using the drag force only.

Figs. 14 and 15 show the standard deviations of the horizontal and vertical wave velocity component. The measured values are obtained from the

experimental data of 50 waves, and the predicted values are based on Eq. (15) with the wave number obtained from Eq. (21). The agreement is good except for the horizontal velocity at x=3.6m. The effect of the vegetation on the wave velocity is small as is the case with the wave data shown in Figs. 9 and 10.

4. Conclusions

A series of laboratory experiments using an artificial seaweed model were conducted to investigate the effects of vegetation on the current and wave fields. Simple theoretical models based on the mixing layer analogy for vegetated flows and linear wave theory are proposed to explain the experimental results.

The current velocity profile resembles that of the mixing layer. The Reynolds stress and turbulent kinetic energy can be estimated by the proposed model. The wave velocity profile based on linear wave theory agrees well with the experimental result because the effect of the vegetation on the wave is small. The drag coefficient obtained from the current data is too large for the wave and current field. It is difficult to describe the effect of the vegetation by the drag force only.

Acknowledgments

The authors gratefully acknowledge Ms. Allison Bridges for preparing the seaweed model. The first author also expresses his gratitude to Profs. Akira Kimura and Yoshiharu Matsumi for providing the opportunity to perform research at the Center for Applied Coastal Research, University of Delaware.

References

Asano, T., H. Deguchi, and N. Kobayashi. 1992. Interaction between Water Waves and Vegetation, Proceedings of 23rd International Conference on Coastal Engineering, ASCE, 2710-2723.

Ghisalberti, M., and H. M. Nepf. 2002. Mixing Layers and Coherent Structures in Vegetated Aquatic Flows, Journal of Geophysical Research, Vol. 107, No. C2, 10. 1029/2001JC000871

Ho, C.-M., and P. Huerre. 1984. Perturbed free shear layer, Annual Review of Fluid Mechanics, 16, 365-424.

Kobayashi, N., A. W. Raichle, and T. Asano. 1993. Wave Attenuation by Vegetation, Journal of Waterway, Port, Coastal, and Ocean Engineering, ASCE, Vol. 119, No. 1, 30-48.

Mendez, F. J., I. J. Losada, and M. A. Losada. 1999. Hydrodynamics Induced by Wind Waves in a Vegetation Field, Journal of Geophysical Research, Vol. 104, No. C8, 18383-18396.

Murota, A. and T. Fukuhara. 1983. Experimental Study on Turbulent Structure in Open-Channel Flow with Aquatic Plants, Proceedings of the Japan Society of Civil Engineers, No. 338, 97-103 (in Japanese).

Nepf, H. M. and E. R. Vivoni. 2000. Flow Structure in Depth-Limited, Vegetated Flow, Journal of Geophysical Research, Vol. 105, No. C12, 28547-28557.

Shimizu, Y and T. Tsujimoto. 1994. Numerical Analysis of Turbulent Open-Channel Flow over a Vegetation Layer Using a k-ε Turbulence Model, Journal of Hydroscience and Hydraulic Engineering, Vol. 11, No. 2, 57-67.

Tamura, H. and K. Nadaoka. 2002. Laboratory Experiments on Hydrodynamic Structure around Flexible and Non-Flexible Seagrass Bed Canopies under Wave Motion, Proceedings of Coastal Engineering, JSCE, Vol. 49 (1), 336-340 (in Japanese).